Microfluidic Cell-phoresis Enabling High-throughput Analysis of Red Blood Cell Deformability and Biophysical Screening of Antimalarial Drugs

Aline T. Santoso[a], Xiaoyan Deng[a], Jeong-Hyun Lee[a], Kerryn Matthews[a], Simon P. Duffy[a], Emel Islamzada[a], Sarah McFaul[a], Marie-Eve Myrand-Lapierre[a], and Hongshen Ma[a,b,c]

a Department of Mechanical Engineering, University of British Columbia, 2054-6250 Applied Science Lane, Vancouver, BC, Canada V6T 1Z4
b Department of Urologic Science, University of British Columbia, Vancouver, BC, Canada
c Vancouver Prostate Centre, Vancouver General Hospital, Vancouver, BC, Canada

SUPPLEMENTAL MATERIALS

Supplemental 1: Multiplexing Error (E_M)

The key design challenge in multiplexing cellular microfluidic cell-phoresis is to ensure a consistent pressure is applied across each deformation microchannel independent from the number of deformation microchannels occupied with cells. The pressure applied across the deformation microchannels (P_D) varies with the number of deformation microchannels occupied with cells (**Supplemental 1**). This phenomenon could be explained by considering the fluid flow in the loading and deformation microchannels in the following two situations: 1) When the deformation microchannels contain no cells, fluid streamlines in the loading microchannels are evenly distributed across the deformation microchannels (**Supplemental 1A**). 2) When one or more of the deformation microchannels are occupied with cells, the fluid flow is blocked in that channel. Consequently, fluid streamlines in the loading microchannel are skewed into the remaining unblocked deformation microchannels (**Supplemental 1B**). The difference between these two situations results in an inconsistency in the flow inside the deformation microchannels, and the resulting deformation pressure, P_D. An equivalent hydrodynamic circuit of these two cases is shown in **Supplemental 1**, where:

- P_{ab}: Pressure across loading and bypass microchannels.
- P_D: Deformation pressure.
- R_D: Hydrodynamic resistance of individual deformation microchannel.
- R_L: Hydrodynamic resi stance of loading microchannels.

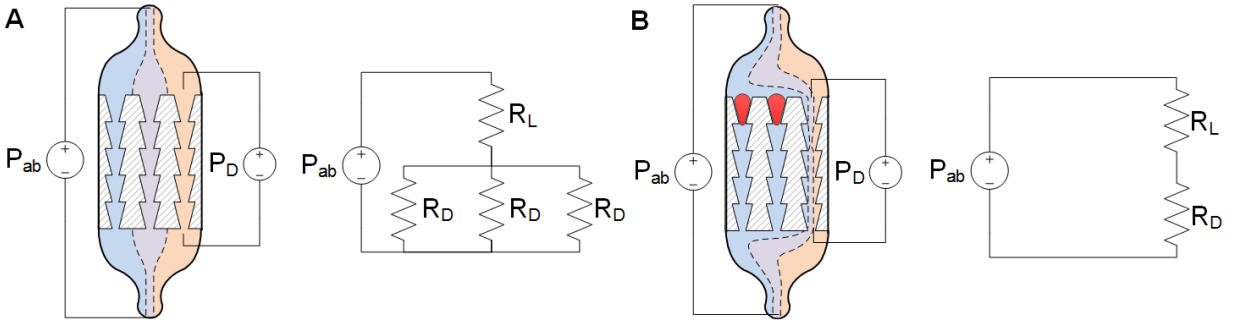

Supplemental 1: Graphic representation of fluid streamlines in the loading and deformation microchannels and its associated hydrodynamic circuit when: (A) All deformation microchannels are unoccupied with cells and (B) only one deformation microchannel is unoccupied.

To estimate the potential error due to microchannel occupancy on the pressure across the deformation microchannels (P_D) for a device with N deformation microchannels, the worst-case pressure difference is considered, which occurs when the deformation microchannels are occupied with a single cell and when the deformation microchannels are completely occupied with cells, which can be estimated as follows:

Deformation microchannels occupied with a single cell:

$$P_{D,1} \approx P_{ab}\left(\frac{R_D}{R_D + (N-1)2R_L}\right) \qquad \text{Equation 1}$$

Deformation microchannels completely occupied:

$$P_{D,N} = P_{ab} \qquad \text{Equation 2}$$

The multiplexing error (E_M) is evaluated as the pressure difference between these two extreme cases (Equation 3) and can be minimized by maximizing the ratio of R_D/R_L based on a target N.

$$E_M = \frac{P_{D,N}}{P_{D,1}} - 1 = (N-1)\frac{2R_L}{R_D} \qquad \text{Equation 3}$$

Supplemental 2: Video of the RBC Deformation Process

Supplemental 3: Image Analysis Software

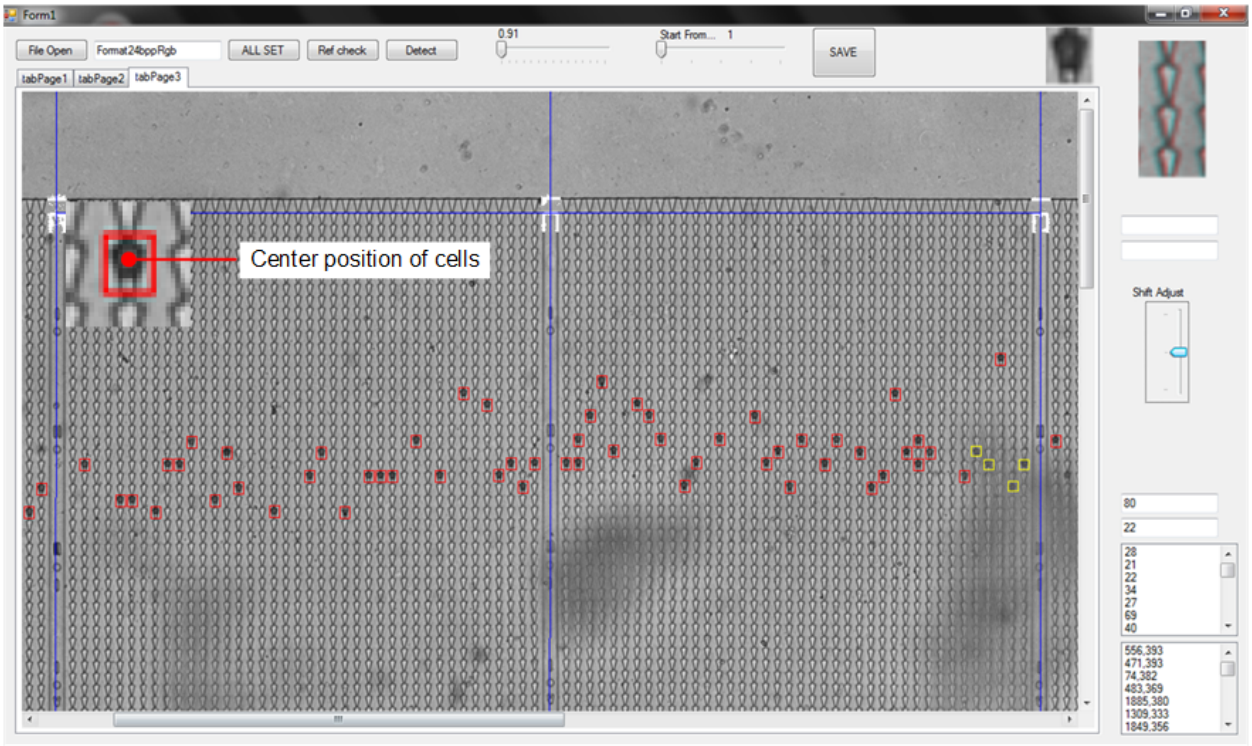

Supplemental 3: Image processing software used to automatically detect RBCs. Red squares indicate automatic detection by the software while yellow squares indicate manual selection by the user. (Inset) The center position of the cell determines its position within the deformation microchannel.

Supplemental 4: Detailed Device Geometries

Supplemental 4: Details of device geometries based on the target cells

Target Cells	Normal RBCs	*P. falciparum* ring-stage iRBCs	*P. falciparum* late-stage iRBCs	Antimalarial drug-treated iRBC
Manifold	4	8	8	8
Number of funnels in a deformation microchannel (N_F)	100	N_{F1}:75 N_{F2}: 75	N_{F1}:75 N_{F2}: 75	N_{F1}:75 N_{F2}: 75
Pressure attenuator ratio (α)	500	500	500	300
Pore Size, W (μm)	1.7	W_1: 1.5 W_2: 1.2	W_1: 2.0 W_2: 1.5	W_1: 2.4 W_2: 1.9
Thickness of deformation microchannel H_F (μm)	3.8 ± 0.1	3.7 ± 0.1	3.9 ± 0.1	4.4 ± 0.1
R_D (Pa.s/m3)	3.91E+17	6.57E+17	4.12E+17	2.15E+17
R_L (Pa.s/m3)	7.12E+13	8.41E+13	8.41E+13	4.40E+13
R_B (Pa.s/m3)	4.26E+12	1.07E+13	1.07E+13	6.48E+12
E_M	4.36%	3.06%	4.87%	4.90%

548 **Supplemental 5: Data Analysis**

549 Due to inherent variability in donors, each experiment was normalized to a sample, which was
550 designated as the control of that experiment (**Supplemental 5**). Data normalization is performed by
551 dividing the position (indicating the deformability) of each cell to the mean and median of the control
552 sample. Samples were normalized to the mean of the control when the expected distribution of the cells
553 is Gaussian, such as with the device validation experiments in **Figure 3**. Parasitized RBCs were also
554 normalized to the mean-value since iRBCs form a very small subpopulation in the sample, resulting in an
555 overall Gaussian distribution. However, iRBCs treated with antimalarials was normalized to the median
556 of the control since the expected population distribution is not Gaussian. This normalized deformability
557 measurement is usually denoted as normalized position of the cells along the deformation
558 microchannel.

559 **Supplemental 5**: Summary of data analysis process for each experiment.

Figure	Experiment	Sample Designated as Control	Normalized To
Figure 3A	Repeated deformations	2 minutes at 20 Pa	Mean-value
Figure 3B	Multiplexing error	Nearly empty	Mean-value
Figure 3C	Oxidatively damaged RBCs	Untreated RBCs	Mean-value
Figure 3D	Applied pressure waveform	Untreated RBCs at 5 Pa	Mean-value
Figure 4	*Plasmodium falciparum* iRBCs	Uninfected RBCs	Mean-value
		Individual sample to produce the cumulative distribution	Mean-value
Figure 5A	Antimalarial-treated iRBCs	DMSO-treated late-stage iRBCs	Median-value

560

561 The small subpopulation of malaria-iRBCs (unsynchronized or ring-stage) becomes progressively
562 stiffer as the parasites mature and also causes bystander injury on the uninfected, exposed RBCs. Hence,
563 to capture the effect of this key subpopulation and to eliminate the effect of uninfected RBCs in the
564 deformability measurement, each sample was normalized to the mean of individual sample, after which
565 the least deformable subpopulation was emphasized in the data analysis by sorting the cells according
566 to its normalized position. The mean of 1% to 100% of the least deformable population fraction was
567 then plotted to obtain a cumulative distribution profile of each sample, which is referred to as the
568 deformability profile of that sample.

569 When more than two groups of samples were investigated, an ANOVA (Analysis of Variance)
570 test was performed, after which an unpaired t-test was used to compare two groups of interest. Mean

with the standard deviation (SD) was plotted for healthy and oxidatively damaged RBCs while median with interquartile range (IQR) was plotted for parasitized RBCs and trophozoites treated with DMSO or drugs. Linear regression was used in **Figure 3A** and **Figure 4D** while non-linear regression was used in section **Figure 3D** to determine the relationship between two parameters. The coefficient of determination (r^2 for linear regression and R^2 for non-linear regression) was used to indicate how good the data fits the statistical model. All statistical analysis was done using GraphPad Prism v6 software (Graphpad Software, US).

Supplemental 6: Effect of Speed on RBCs Shape

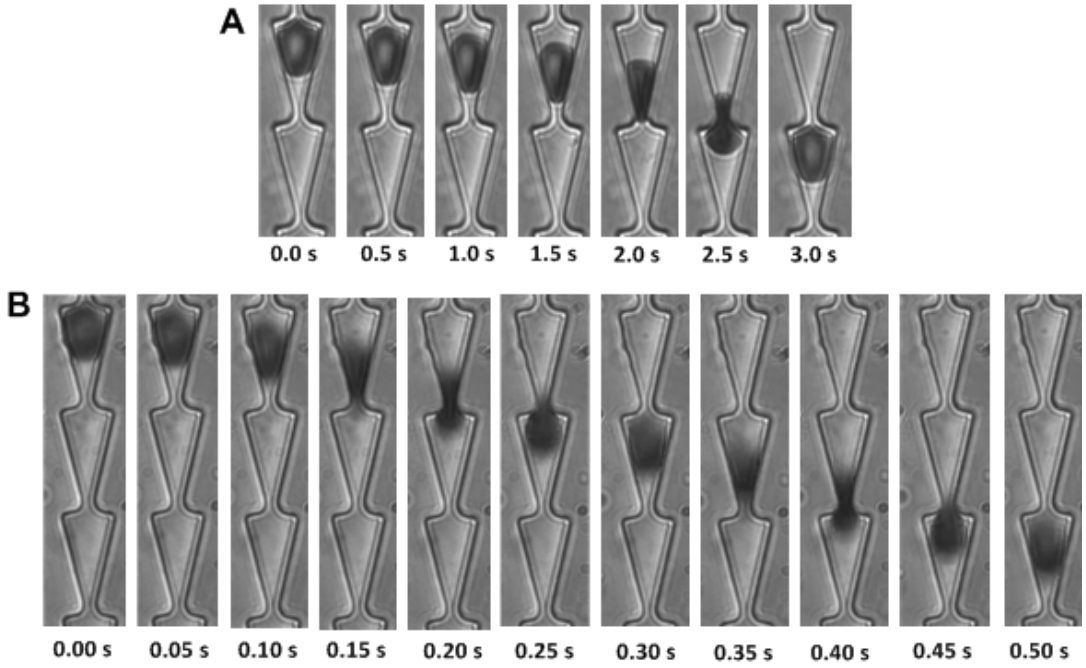

Supplemental 6: Shape of an RBC during deformation process: (A) at 15 Pa, the RBC goes back to its normal discoid shape after each deformation; (B) at 120 Pa, the RBC remains in its deformed, "bullet" shape, resulting in a loss of device capability to resolve the difference in RBC deformability.

583 **Supplemental 7: Malaria data**

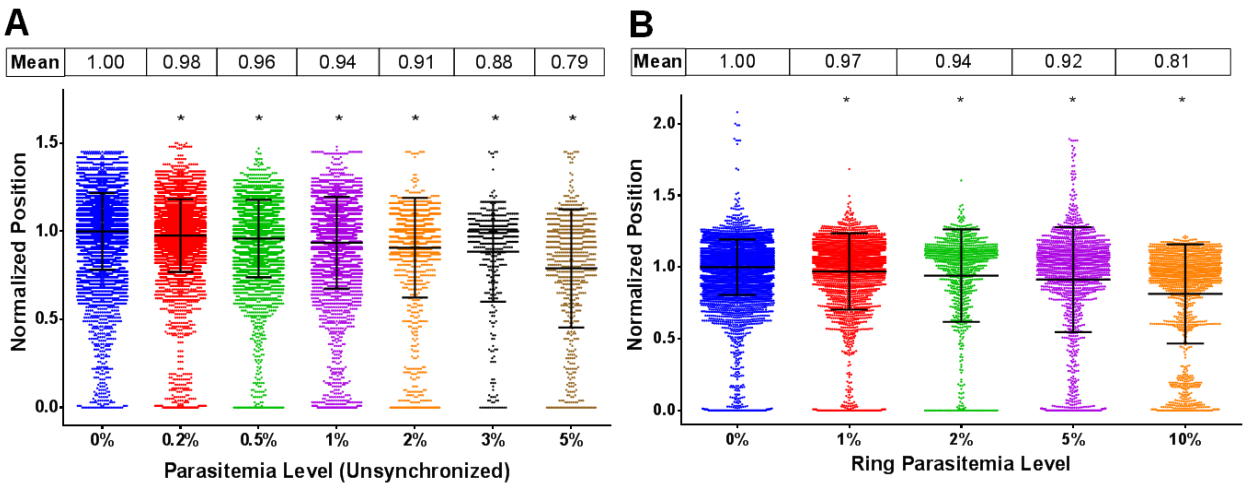

584
585 **Supplemental 7: (A)** The deformability patterns of RBCs parasitized with unsynchronized *P. falciparum*. Each
586 sample is normalized to the mean of the control. The normalized mean of the sample decreases with increasing
587 parasitemia level, with $p<0.0001$ for (*) with respect to control ($n=8575$ for control and an $n\geq500$ for 3%
588 parasitemia level). **(B)** The deformability patterns of RBCs parasitized with synchronized *P. falciparum* at ring-stage
589 show decreased mean normalized position occuring with increasing parasitemia level with $p<0.0001$ for (*)
590 ($n=9074$ for control and an $n\geq978$ for 2% parasitemia level).

Supplemental 8: Antimalarials negative control using uninfected RBCs

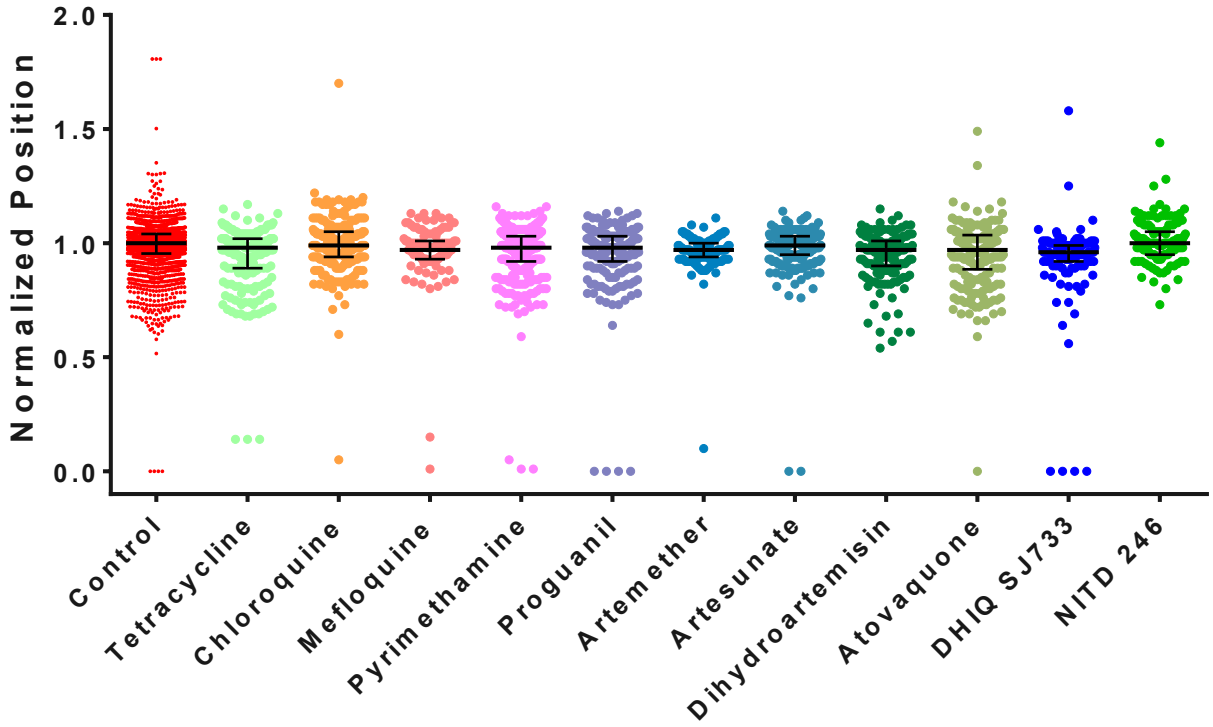

Supplemental 8: Deformability of normal RBCs treated with ≥ 4 x EC_{50} concentration of antimalarial drugs showing no appreciable difference relative to control.

596 **Supplemental 9: Detailed result for antimalarial drug treatments**

597 **Supplemental 9**: Individual concentrations and normalized deformability values for various antimalarial drug
598 treatments (n=616 for control and n≥100 for iRBCs)

Drug Name	Concentration (≥ 4 × EC50)	Number of RBCs	Median	% decrease vs. DMSO	p-value
Tetracycline	100 µM	245	1.00	0	0.54
Chloroquine	1 µM	502	0.66	34	<0.0001
Mefloquine	1 µM	281	0.67	33	<0.0001
Pyrimethamine	20 nM	267	0.55	45	<0.0001
Proguanil	100 µM	205	0.59	41	<0.0001
Arthemether	8 nM	364	0.24	76	<0.0001
Artesunate	10 nM	270	0.82	18	<0.0001
Dihydroartemisinin	20 nM	233	0.61	39	<0.0001
Atovaquone	250 nM	100	0.56	44	<0.0001
(+)-SJ733	1.08 µM	307	0.01	100	<0.0001
(-)-SJ733	1.08 µM	153	1.02	-2%	0.1
NITD246	3.6 nM	369	0.00	100	<0.0001

599